The Relationship between Satellite Measured Convective Bursts and Tropical Cyclone Intensification

JOSEPH STERANKA

General Software Corporation, Landover, MD 20785

EDWARD B. RODGERS

Laboratory for Atmospheres, NASA/Goddard Space Flight Center, Greenbelt, MD 20771

R. CECIL GENTRY

Department of Physics and Astronomy, Clemson University, Clemson, SC 29631

(Manuscript received 21 August 1985, in final form 18 February 1986)

ABSTRACT

The relationship between the mean temperature of the top of the cloud canopies and the future maximum winds of Atlantic Ocean tropical cyclones is analyzed. The area-average cloud top temperatures from 309 observations of 12 tropical cyclones which occurred during 1974–79 were compiled from infrared measurements made by Geostationary Operational Environmental Satellites. Maximum winds were obtained from best track records.

The satellite measurements showed that prolonged surges of intense convection developed in the near region surrounding the depression centers before the maximum winds initially increased. Subsequent weakening of the convection occurred but was frequently followed by new surges of intense convection. It was found that when these prolonged surges of intense convection lasted for 9 or more hours, and the filtered (6-h running mean) area-average cloud top temperature within 222 km of the tropical cyclone centers was 238 K or less, that the maximum winds of the tropical cyclones increased by 5 m s^{-1} or more within 24 h later, 71% of the time. However, when intense convection was not present, similar maximum wind increases occurred only 37% of the time.

The future maximum winds were compared with both the filtered area-average cloud top temperatures measured during the strong convective surges and the storm's intensities at the filtered temperature times using multiple linear regression. The correlation was found to be 0.771 for moderate/strong storms (storm intensity of 26 m s^{-1} or more) and 0.610 for weak storms (storm intensity of less than 26 m s^{-1}). The relationships are statistically significant at the 0.0005 and 0.05 levels, respectively, and the lag time is near 24 h. The standard error of the regression is 5.7 and 6.2 m s^{-1}, respectively. Statistical tests made to determine the quality of expected performance suggest that predictive equations will yield maximum wind intensities within 3 and 4 m s^{-1}, respectively, of the standard error of the regression 95% of the time. In an independent test, the standard deviation of the error of the predicted maximum winds of moderate/strong storms was 8 m s^{-1}, or well within the expected bounds.

1. Introduction

The equivalent blackbody temperatures (T_{BB}) of cloud tops obtained with the geosynchronous meteorological satellites provide immediate information about the strength and distribution of the convection in tropical cyclones. While the temperatures of the cloud tops near the tropical cyclone centers can be used as an index of convection, they may also provide information about the relative magnitude of the latent heat energy being released. This energy is the primary fuel of tropical cyclones (Dunn and Miller, 1960) and it has an important role in storm intensification.

Latent heat energy becomes available in abundance as the warm moist tropical air ascends and condenses in the major cumulus towers of the tropical cyclones. The latent heat release (LHR) appears to be the energy source for the driving mechanisms which bring moisture and momentum into and mass out of the storm system (Riehl, 1954). The associated organization of convective cells into cyclonic bands helps to maintain the nonlinear cooperative interaction between the cyclone and cumulus scales (Ooyama, 1982; Schubert and Hack, 1982a,b) and the local mass recycling (Gray and Shea, 1973; Gray, 1979) that is necessary for enhancing surface energy flux. As these, as well as other forces are at work, the maximum winds increase and the eyewall, or even concentric eyewalls (Willoughby et al., 1982), forms. Then even greater maximum winds may be experienced. The convective process and its associated LHR are fundamental to the complex process which leads from organized mesoscale convection to the violent hurricane. In theoretical-numerical model experiments (Kurihara and Tuleya, 1974;

Rosenthal, 1978) which simulate tropical cyclone maintenance and development, the highest winds followed the maximum convection by 24–72 h. Satellite measurements of convective processes of Pacific Ocean tropical cyclones using LHR derived from measurements of the electrically scanning microwave radiometer on Nimbus-5 (Adler and Rodgers, 1977; Rodgers and Adler, 1981), and the mean T_{BB} of the cloud tops measured with the infrared (11.5 μm) window channel of Numbus-4 and -5 used as an index of LHR (Gentry et al., 1980) show that a strong statistical relationship exists between the convective indices and the maximum winds of the tropical cyclones 24–48 h later. Because such strong relationships exist, a knowledge of the relative strength of the LHR index (mean T_{BB} of the cloud tops) (or its change) becomes highly useful in deliberations on future tropical cyclone intensity.

In this study the high temporal resolution measurements of the geosynchronous satellite are used to analyze the patterns of the deep convection of tropical cyclones, to develop the statistical relationship between the convection and the future maximum winds, and to demonstrate approaches for applying the cloud top temperature measurements in forecasting storm intensity. Since the geosynchronous satellites offer greater temporal resolution than that of the lower, polar-orbiting satellites, new information about the onset of short- and long-term convective activity is expected to be gained.

2. Data

The data set is comprised of the area-average T_{BB} measurements of 309 cloud canopies and the maximum winds of 12 Atlantic Ocean tropical cyclones which occurred during 1974–79. The satellite measurements of this study set are limited to those obtained in storms which were moving with a westerly zonal component and were not considered to be interacting with extratropical systems. The area-average T_{BB} measurements compiled at 3-h intervals were made with the infrared channel (11.5 μm) of the visible and infrared spin-scan radiometer (VISSR) of the Geostationary Operational Environmental Satellite (GOES). The maximum wind speeds were obtained from the best track records compiled by the National Hurricane Center.

Each area-average T_{BB} value is the average of all of the data points within 222-km radius of the tropical cyclone center at a particular time. The observational points within the eye or of cloud tops obscuring the eye, though included in the area-averages, contribute negligibly (<0.05%) to the population of any single area-average T_{BB} value. Only observations of tropical cyclones >111 km from land are included in the data set. Although area-average T_{BB} was obtained at essentially 3-h intervals, some data gaps resulted; the data gaps of $\leq$12 h were filled at 3-h intervals using linear interpolation. A low-pass filter (6-h running means) was used to smooth out the frequent short-term oscillations of the area-average T_{BB} which appeared in the temporal profiles; however, the semidiurnal and diurnal oscillations (Steranka et al., 1984) still remained. The T_{BB} compilation was made using the Atmospheric and Oceanographic Information Processing System (AOIPS) at Goddard Space Flight Center.

The data are stratified into two sets: an exploratory (dependent) set consisting of 232 observations from eight tropical cyclones and a verification (independent) set of 77 observations from four tropical cyclones. This stratification permits independent testing of predictive approaches developed with the exploratory set.

3. Results and discussion

a. Qualitative findings

The time trends of the 6-h running mean area-average T_{BB} (6-h RMT) of the inner canopy and the maximum winds for selected periods of three tropical cyclones (Hurricane Faye, 1975; Hurricane Fifi, 1974; and Tropical Storm Elaine, 1974) are shown in Fig. 1. These cases represent the three commonly found temporal 6-h RMT patterns: Faye, a hurricane with multiple major surges of strong convection; Fifi, a hurricane with brief minor surges followed by a major surge of strong convection; and Elaine, a tropical storm with a strong surge of convection followed by a brief period with a lesser surge. The periods of strongest convection, delineated as convective bursts (CVB), are associated with the lower (colder) 6-h RMT which show a decreasing (cooling) trend. The profiles show that the maximum winds of the tropical cyclones first began to increase after the CVB's developed. Additionally, the greatest storm intensity was reached after the strongest convection (lowest 6-h RMT) was observed.

The CVB is a period of intense convection during which LHR becomes available in great abundance. Because of the LHR/maximum wind relationship, knowledge of the CVB's existence (or absence) provides information about the LHR which is useful for determining the likelihood of storm intensity change and an intensity outlook can be provided with greater confidence.

The conditions for defining the CVB were established by reviewing the temporal profiles of the 6-h RMT of the tropical cyclones of the exploratory set only. The periodic surges of reduced 6-h RMT were found to vary in duration and magnitude. These surges were considered to be associated with convective periods of varying duration and strength. The most pronounced surges were characterized with cooling trends where the 6-h RMT was <250 K and where the initial 9-h decrease of the 6-h RMT was $\geq$5 K. During the initial 9-h period, no single intervening 6-h RMT value exceeded its immediate predecessor by >1 K. Further

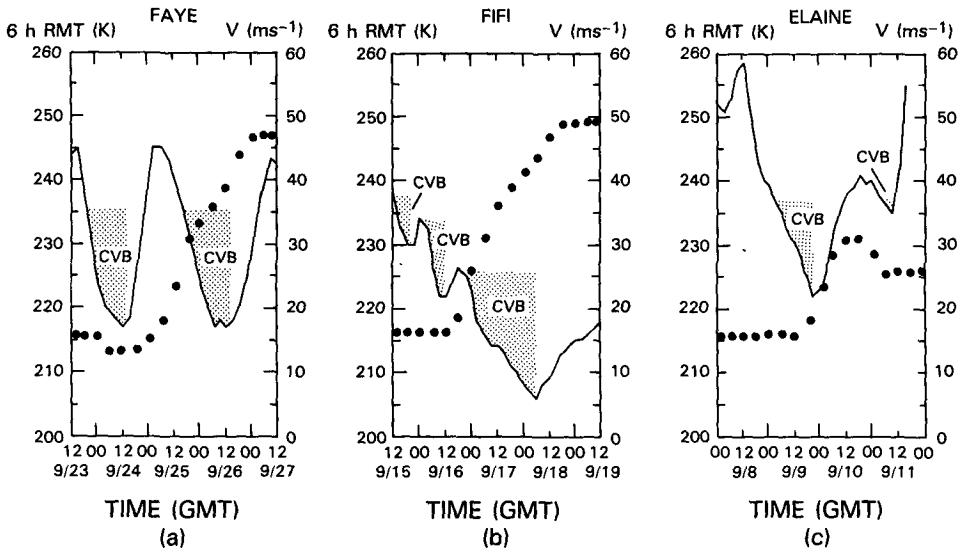

FIG. 1. Time trends of the 6-h RMT (solid) of the inner cloud canopy and the maximum winds (dotted) for (a) Hurricane Faye, 1975; (b) Hurricane Fifi, 1974; and (c) Tropical Storm Elaine, 1974. The convective burst (CVB) periods are shaded.

decreases in the 6-h RMT frequently continued after the initial cooling trend was established. The cooling trends were found to end abruptly and the end was characterized by an increase of >1 K of the 6-h RMT over the value of its immediate predecessor. The higher valued 6-h RMT of 235–249 K were useful for establishing the cooling trend but are not associated with the stronger convection believed to provide the greater abundance of LHR. Therefore, a qualitative judgement was made to use these higher values for establishing the existence of a cooling trend but not to consider all of the higher values as a part of the CVB. By removing the upper 10% of the 6-h RMT values of <250 K, only values of ≤238 K remained. These findings and judgements led to ascribing the term "*convective burst*" *(CVB) to the portion of the cooling trend where the 6-h RMT is ≤238 K and where no single succeeding 6-h RMT exceeds its immediate predecessor by >1 K.*

Following the CVB the 6-h RMT showed a warming trend but in some cases there was a renewed surge of strong convection which could be established by again applying the cooling trend criteria (i.e., ≥5 K decrease of the 6-h RMT in a 9-h period without intervening increases of >1 K). However, it is sometimes found that during a warming trend strong convection is still present. This category of convection will be defined as *unsettled and it occurs when the 6-h RMT ≤238 K and there is a warming trend. Weak convection is considered to be present only when the 6-h RMT is ≥239 K independent of the trend.*

One or more CVB's were found in the temporal 6-h RMT profile of each of the tropical cyclones of the study set; a total of 21 CVB's were identified. The first CVB was found to develop initially when the tropical system was at the depression stage (maximum wind <18 m s^{-1}). Although only one CVB was sometimes observed, as many as four CVB's developed during the life history of some tropical cyclones. The intensity of each CVB was usually greater (lower 6-h RMT) than that of its predecessor. The reoccurrence of CVB's were observed 1) in storms passing over land (the Yucatan Peninsula and large Caribbean Islands) where the intense convection weakened upon landfall but redeveloped as open water was reached; 2) in storms located at subtropical (including the Gulf of Mexico) or in middle latitudes for several days where transitory midlatitude systems may be affecting the storms; and 3) in the case of Faye (1975) as the storm moved into the proximity of a tropical upper tropospheric trough (Sadler, 1976).

The occurrence of multiple CVB's is suggestive of the presence of transitory upper-level divergence fields which couple or uncouple with the tropical cyclone's upper outflow to produce conditions favorable (CVB develops) or unfavorable (CVB weakens or ends) for convective development. A single CVB of extended duration may be the result of a favorable divergence field which appears in the tropical cyclone's environment, couples, and moves along in the same general direction of the storm.

b. Quantitative results

1) STATE OF CONVECTION VS FUTURE MAXIMUM WINDS

The review of the 6-h RMT and maximum wind profiles of the tropical cyclones of the study set revealed, also, that the maximum winds increased with greater frequency after a CVB developed than after weak convection was observed. Although there appeared to be

varying lag times, from storm to storm, between onset of strong convection and increase in the maximum wind, a common lag time of 24 h after 6-h RMT time was used to determine the frequency at which a significant (≥ 5 m s^{-1}) higher maximum wind was observed following the satellite observations made during each of the three convective conditions: CVB, weak, unsettled. A compilation was made for both the exploratory and the verification sets. In Table 1 a summary of the wind change compilation shows the frequency at which the maximum wind was ≥ 5 m s^{-1} higher at 24 h after the maximum wind observed at the 6-h RMT time. The results are stratified by storm intensity (V) at the 6-h RMT time: weak, $13 \leq V < 26$ m s^{-1}; moderate, $26 \leq V \leq 41$ m s^{-1}; strong, $V > 41$ m s^{-1}.

The results shown in Table 1 for the exploratory and verification sets indicate that the frequency of occurrence of maximum wind increase ≥ 5 m s^{-1}, 24 h after the 6-h RMT time during the CVB's is high (0.62, 1.0 and 0.75, 0.81) for weak and moderate storms respectively. The maximum winds of the strong storms are not higher with such great frequency. The frequency is low following periods of weak convection: 0.34 and 0.30 for weak storms, 0.38 and 0.33 for moderate storms, and 0 and no sample for strong storms. The results for the unsettled condition are mixed, showing higher winds with frequencies of 0.53 and 1.0 for weak storms, 0.30 and 0.10 for moderate storms, and 0.38 and 0 for strong storms. By combining the frequencies of all intensity categories of both study sets there is found a high frequency (0.71) of higher maximum winds following the CVB's, but only frequencies of 0.33 and 0.4 following weak and unsettled conditions, respectively.

The statistical results shown in Table 1 provide a useful climatology which suggests that there is a good probability of correctly estimating that a storm will or will not intensify, when there is knowledge of the character and strength of the storm's convection. By applying the character and strength in a predictive sense, a storm would be expected to have maximum wind ≥ 5 m s^{-1} higher, 24 h after the 6-h RMT during a CVB but would not have gained higher maximum winds following the 6-h RMT at all other times. Such an outlook was prepared and the results are shown in Table 2. Additionally, the outlook for storm intensity change was prepared using persistence and SHIFOR (Jarvinen and Neumann, 1979) techniques. The persistence techniques are widely used for estimates of future maximum wind intensity. Persistence techniques predict no change (NC) in the future maximum wind during the 24-h period, or persistence of change (PC) where the maximum wind during a subsequent 24-h period will change by an amount equal to the change observed during a past equivalent period. The SHIFOR technique uses seven climatological parameters to forecast 24-h intensity change with an equation developed by multiple regression. A correct outlook was assigned for NC when the intensity increase was <5 m s^{-1}; and a correct outlook was assigned for PC and SHIFOR when the predicted increase was <5 m s^{-1} and the observed increase was <5 m s^{-1}, or when the predicted increase was ≥ 5 m s^{-1} and the observed increase was ≥ 5 m s^{-1}. The outlooks were verified using intensity changes obtained from best track maximum wind records. The frequencies for correct outlook for each of the prediction methods for each convective state are compared in Table 2.

The superiority of the character of convection outlook over the persistence and SHIFOR outlooks during a CVB is evident: frequency of 0.71 vs 0.20 and 0.29 for persistence and 0.42 for SHIFOR for the exploratory set and 0.72 vs 0.41 and 0.16 for persistence and 0.30 for SHIFOR for the verification set. The PC and SHIFOR approaches yielded best results during periods of weak convection. The NC approach yielded results equal to the character of convection during weak and unsettled convection but SHIFOR was best with the verification set. By combining all convective states of both data sets the frequencies of correct outlook are 1) PC, 0.45; 2) NC, 0.46; 3) SF, 0.55; and 4) CC, 0.67. The state of convection outlook is an improvement of 49% over the PC, 46% over the NC, and 22% over SF.

TABLE 1. Frequency at which the maximum wind (V) was ≥ 5 m s^{-1} higher 24 h after the 6-h RMT time for observations made during CVB's, periods of weak (WC) and unsettled (UN) convection for the exploratory (EX) and verification (VF) sets.

Storm set	Storm intensity at 6-h RMT time*	Frequency of ≥ 5 m s^{-1} higher maximum wind			Number of observations		
		CVB	WC	UN	CVB	WC	UN
EX	Weak, $13 \leq V < 26$	0.62	0.34	0.53	42	41	17
EX	Moderate, $26 \leq V \leq 41$	0.75	0.38	0.30	64	13	33
EX	Strong, $V > 41$	1.00	0	0.38	6	3	13
VF	Weak, $26 \leq V < 41$	1.00	0.30	1.00	5	10	10
VF	Moderate, $26 \leq V \leq 41$	0.81	0.33	0.10	21	9	10
VF	Strong, $V > 41$	0.14	—	0	7	—	5

* Units of V are m s^{-1}.

TABLE 2. Comparison of the frequency of the correct 24-h outlook of the maximum wind change obtained by using the character of convection (CC) as the predictor, using no change (NC) and persistence of change (PC) persistence prediction techniques, and using the SHIFOR (SF) technique for the three convective states: intensifying (CVB), weak (WC), and unsettled (UN).

Data set	Character of convection	PC	NC	CC	SF	Number of observations
EX	CVB	0.20	0.29	0.71	0.42	112
EX	WC	0.84	0.67	0.67	0.84	57
EX	UN	0.46	0.62	0.62	0.46	63
VF	CVB	0.41	0.16	0.72	0.30	32
VF	WC	0.79	0.68	0.68	0.95	19
VF	UN	0.44	0.56	0.56	0.72	25

2) MAGNITUDE OF THE 6-H RMT VS MAGNITUDE OF FUTURE MAXIMUM WINDS

Since it is desirable to make definitive quantitative predictions of storm intensity, the relationship between the magnitudes of 6-h RMT, the storm intensity at 6-h RMT time and the future maximum winds was analyzed. As a first step, the relationship between the area-average T_{BB} and the future maximum winds was analyzed. Numerous candidates were considered. In this respect, the area-average T_{BB} of various radii from 111 to 555 km of center, standard deviation, the 6-h RMT, the area-average T_{BB} change, and areal size of the area-average T_{BB} at fixed threshold levels ($\leq$210 K, $\leq$220 K, $\leq$230 K) were compared with present, past, and future winds and their changes. Certain candidates produced superior results within a given storm, but the results did not prevail for the entire exploratory set. *The best results were obtained between the magnitude of the 6-h RMT observed during the CVB (as the convection was increasing) and the maximum winds at some future time.*

It could be easily seen from the 6-h RMT and maximum wind profiles that there was a difference in the lag time between convective increase during a CVB and the future maximum wind increases from storm to storm, or even within the same storm. Since a common lag time was not apparent, it was decided to determine the least-squares fit between the 6-h RMT of each CVB and the maximum wind at all logical future time periods; then the time at which the best least-squares fit occurred for each CVB would determine the lag time. The data pairs of 6-h RMT and future maximum wind from each CVB would become a part of a larger data set developed from the best fit pairs of all CVB's.

The 6-h RMT at 3-h intervals from the time of the beginning of each CVB (when 6-h RMT first decreased to $\leq$238 K) to the time of the end of the CVB (i.e., where 6-h RMT exceeds its immediate predecessor T_{BB} by >1 K) some hours later were compared to maximum winds 9 to 48 h later. The comparison was made for each 3-h interval (i.e., 9 h, 12 h, 15 h, 18 h, etc.); the best least-squares fit was determined. The data pairs that had the best least-squares fit also determined the lag time between the magnitude of the 6-h RMT and the future maximum wind. For example, in Fig. 1a, the 6-h RMT for the period of increasing convection between 1800 GMT 23 September (when the 6-h RMT had first decreased to $\leq$238 K) to 1500 GMT 24 September (at the time of the end of the CVB) had a best least-squares fit with the maximum winds 24 h later between 1800 GMT 24 September to 1500 GMT 25 September. Later, during a second CVB, the 6-h RMT from 1800 GMT 25 September to 1500 GMT 26 September has a best least-squares fit with the maximum winds 18 h later from 1200 GMT 26 September to 0900 GMT 27 September. It can be seen from this example that the lag time that corresponded to the best least-squares fit was not always identical. This was true throughout the study set. The best fit 6-h RMT and future maximum wind lag time varied from 12 to 39 h.

The entire set of data pairs from all of the CVB's were analyzed as a single set and the correlation of the 6-h RMT with the future maximum wind was found to be −0.693. A scatter diagram of the data pairs is shown in Fig. 2. A stronger relationship (−0.757) was found to exist between the 6-h RMT and the future maximum winds of moderate/strong storms (storm intensity of $\geq$26 m s^{-1} at the 6-h RMT time); the relationship of the weak storms (storm intensity of <26 m s^{-1}) was −0.387. The average lag time and its standard deviation was also determined. The relationships for the entire set and the moderate/strong storms are significant at the 0.0005 level; for the weak storms, at the 0.01 level (single tail, student t test). The results of the relationships are shown in Table 3. The 6-h RMT during periods of weak and unsettled convection has only a weak statistical relationship with the future maximum winds.

In the final step toward obtaining predictive equations for quantitative estimates of the storm's future intensity, the relationship of the future maximum wind with the 6-h RMT observed during the CVB's together with the storm's intensity at the time of the 6-h RMT was developed for the above storm categories. The equations obtained from a multiple regression analysis are

$$V_{all} = 69.3882 - 0.2651T + 0.9592V \quad (1)$$

$$V_w = -2750.4729 + 24.7575T - 0.0554T^2 + 0.899V \quad (2)$$

$$V_{ms} = 155.9237 - 0.567T + 0.3961V \quad (3)$$

where V_{all}, V_w, V_{ms} are the predicted wind intensity at mean lag time for all storms, weak storms, and moderate/strong storms, respectively; T is the 6-h RMT of the cloud tops within 222 km radius of the tropical cyclone center observed during a CVB; and V is the storm intensity at the 6-h RMT time. Equation (1) is

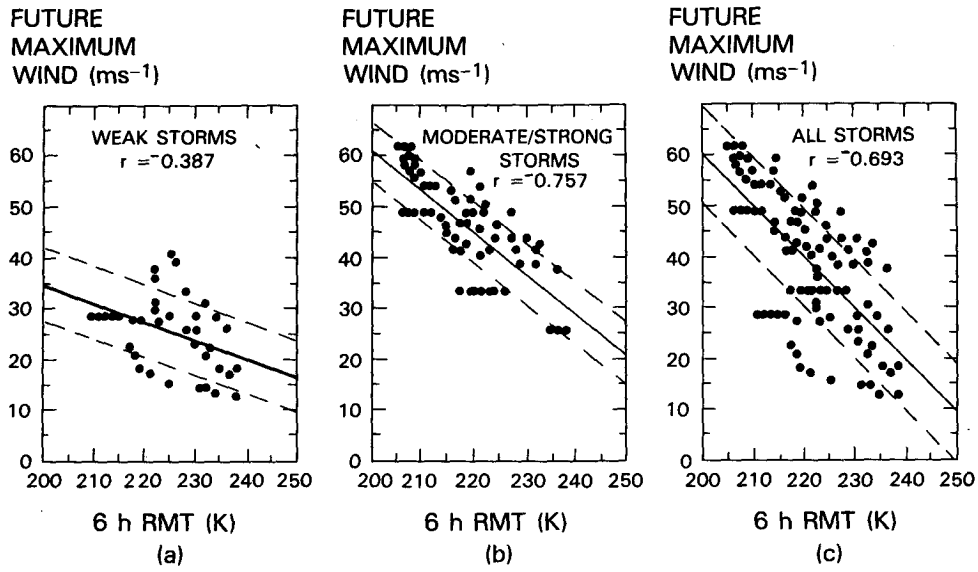

FIG. 2. Scatter diagrams of the future maximum wind vs the 6-h RMT for (a) weak storms, (b) moderate/strong storms, and (c) all storms. The regression lines (solid) and the standard deviation lines (dashed) are shown.

applied when the storm intensity (V) at the 6-h RMT time is $\geqslant 13$ m s^{-1}, Eq. (2) when $13 \leqslant V < 26$ m s^{-1}, and Eq. (3) when $V \geqslant 26$ m s^{-1}. The Eqs. (1) and (3) are significant at the 0.0005 level, and Eq. (2) is significant at the 0.01 level (single tail, student t test). A summary of the statistics of the regression is provided in Table 4.

A two sided statistical test was made to determine how well the equations are likely to perform (Neter et al., 1978). Such testing is useful in answering two questions which arise: 1) What is the expected outcome? and 2) Is the sample size large enough? The results of this test at the 95% confidence level suggest that the mean forecast error for the categories all, weak, moderate/strong will not exceed 3, 5, 4 m s^{-1} of the standard error of the estimates, respectively. An increased sample size would considerably reduce the expected error, at this confidence level, assuming that there was little increase in the standard error of the estimate.

The predictions obtained with the regression analysis of the exploratory set were compared with the predictions developed using persistence and SHIFOR techniques. The errors resulting from each technique are summarized in Table 5. This summary shows that the predictive equations produced smaller errors than those obtained using persistence (standard error of 0.3–2.4 m s^{-1} less), and SHIFOR (3.4–5.5 m s^{-1} less).

The predictive equations were used with the 6-h RMT within a 222-km radius of the storm center of the verification set observed during each CVB to determine the quality of the predictions with independent data. Persistence and SHIFOR predictions were also prepared. The results are summarized in Table 6 for the moderate/strong storm cases only; there were not a sufficient number of weak storm cases for a significant test. At 24 h, Eq. (3) yielded smaller errors than NC, PC, and SF forecasts (1.8, 8.1, and 2 m s^{-1}, respectively). The NC predictions had lower standard devia-

TABLE 3. Summary of the statistical relationship of the 6-h RMT with the future maximum winds (exploratory set only). Storm intensity at 6-h RMT time is V.

Statistic	Intensity category		
	All storms $V \geqslant 13$ m s^{-1}	Weak $13 \leqslant V < 26$ m s^{-1}	Moderate/strong $V \geqslant 26$ m s^{-1}
Correlation coefficient	−0.693	−0.387	−0.757
Standard error of estimate (m s^{-1})	8.4	6.9	5.9
Mean lag time (h)	23.2	22.1	23.8
Standard deviation of lag (h)	7.2	7.4	7.0
Number of cases	106	36	70
t statistic	9.81	2.45	9.54
F statistic	175.41	5.98	91.08

TABLE 4. Summary of the statistics of the regression for the predictive equations.

Statistic	Intensity category		
	All	Weak	Moderate/ strong
Multiple correlation coefficient	0.879	0.610	0.771
Error of the regression (m s^{-1})	6.3	6.1	5.8
F statistic	175.41	6.33	49.05

tions of error than those of Eq. (1) but the predictions are biased >5 m s^{-1} too low. It is particularly significant that the standard deviation of error of Eqs. (1) and (3) predictions of 9.1 and 8 m s^{-1}, respectively at 18 h (within the time lag standard deviation) are well within the expected limits (6 m s^{-1} ± 3 m s^{-1} and 6 m s^{-1} ± 4 m s^{-1}) developed with the size and risk test of the exploratory set. Equation (3) was developed for moderate/strong storms only and performed better than Eq. (1) which was developed for use with storms of any intensity.

A statistical test of the confidence interval of the predictive equation results from the exploratory and verification sets was made (Neter et al., 1978). These results show that there is a 95% probability that the mean error of the forecasts using the predictive equations will not exceed the difference of the mean errors of the sets by >3.1 m s^{-1}. As long as the underlying assumptions of the tests apply, particularly normal distribution, this test and the size and risk tests discussed earlier are considered valid. Their results suggest that the predictive equations will perform well within the expected 95% limits.

3) POSSIBLE OPERATIONAL USAGE OF THE PREDICTIVE METHODS

In an operational mode, there is no a priori knowledge of the CVB and the forecaster must wait until the criteria of the CVB are met before applying the predictive methods discussed. It is possible that by carefully monitoring the satellite imagery of the tropical cyclone for improved cloud organization together with the temporal profile of the 6-h RMT that the onset of the CVB might be established earlier. In any case, when the 6-h RMT values fall to 238 K or less, the forecaster should be watchful for continued increased convection. Obviously, the longer the trend of decreasing 6-h RMT, the more confident the forecaster can be that a CVB has developed. Once satisfied that a CVB exists, the predictive methods discussed earlier could be applied and storm outlook prepared.

TABLE 5. Comparison of the errors of predicted maximum winds from predictive equations, persistence, and SHIFOR techniques (exploratory set only).

Storm category	Method	Standard error of estimate (m s^{-1})	Mean absolute error (m s^{-1})	Number of cases
All	Eq. (1)	6.3	5.3	106
Weak	Eq. (2)	6.1	4.5	36
Mdt/strong	Eq. (3)	5.8	4.7	70
All	NC	6.6*	9.9*	106
Weak	NC	6.8*	8.5*	36
Mdt/strong	NC	6.3*	10.7*	70
All	PC	7.9	6.6	106
Weak	PC	8.5	7.8	36
Mdt/strong	PC	7.5	6.0	70
All	SF	9.7*	8.0*	106
Weak	SF	11.6*	9.3*	36
Mdt/strong	SF	10.1*	8.6*	70

* Mean prediction errors are biased >5 m s^{-1} too low.

4. Conclusions

The area-average T_{BB} of the cloud canopies within 222 km of the center of tropical cyclones are valuable indicators of the strength and distribution of the storm's inner convection and of the availability of latent heat energy. The high temporal frequency of the measure-

TABLE 6. Comparison of the errors (m s^{-1}) of predicted maximum winds from predictive equations, persistence, and SHIFOR techniques for moderate/strong storms (verification set only).

Method:	Time after 6-h RMT								
	18 h			24 h			30 h		
	Mean	Standard deviation	Mean absolute	Mean	Standard deviation	Mean absolute	Mean	Standard deviation	Mean absolute
Eq. 1	1.1	9.1	6.8	1.6	11.8	8.4	2.5	13.3	9.9
Eq. 3	−2.2	8.0	6.3	−1.7	9.6	7.4	−0.8	10.3	8.0
NC	−6.7	8.6	9.2	−6.2	11.4	11.0	−5.2	13.1	12.4
PC	3.9	13.3	10.1	16.9	17.7	20.5	10.7	20.5	16.4
SF				−4.4	11.6	9.3			
Number of cases		28			28			28	

ments from GOES makes it possible to recognize the onset of the intense convective bursts. The strong bursts, or CVB, which develop may result from the favorable coupling of the storm's upper outflow with divergence fields transiting or remaining within the tropical cyclones environment. A lag time between the onset of deep convection and the onset of maximum wind increase is particularly evident and follows the theoretical logic of the latent heat and kinetic energy relationship.

In an applied sense, a 67% frequency of correct qualitative estimates of future maximum wind changes was obtained by using the state of convection as the predictive parameter. Additionally, the predictive equations produced good quality estimates of the magnitude of the future maximum wind. Both forecast approaches yielded lower errors of future maximum wind estimates than the errors resulting from the persistence and SHIFOR techniques. The results suggest that once the criteria for the CVB have been met, confidence for predicting tropical cyclone intensification is high and quality of the forecast is likely to be improved over that of persistence or SHIFOR.

Acknowledgments. The authors appreciate the dedicated assistance of the computer specialists, particularly Mr. Ray Morris, in the compilation of the T_{BB} data from the more than 1400 computer tapes. The typing of the several drafts by Mrs. Cora Lee Sawyer and Ms. Kelly Wilson is appreciated. The constructive suggestions provided by Drs. Joanne Simpson and Robert Adler were highly useful. The reviews of draft material by Drs. Peter Black, William Gray, John McBride, Hugh Willoughby and Rear Admiral William Kotsch provided welcome constructive comments. The review of the statistics made by Dr. Ronald L. Biondini was invaluable in the preparation of this manuscript. The support for this research was provided by NASA/Goddard Space Flight Center, Laboratory for Atmospheres.

REFERENCES

Adler, R. F., and E. B. Rodgers, 1977: Satellite-observed latent heat release in a tropical cyclone. *Mon. Wea. Rev.*, **105,** 956–963.

Dunn, G. E., and B. I. Miller, 1960: *Atlantic Hurricanes,* Louisiana State University Press, 123 pp.

Gentry, R. C., E. Rodgers, J. Steranka and W. Shenk, 1980: Predicting tropical storm intensity using satellite measured equivalent blackbody temperature of cloud tops. *Mon. Wea. Rev.*, **108,** 445–455.

Gray, W. M., 1979: Hurricanes: Their formation, structure and likely role in the tropical circulation. *Meteorology Over the Tropical Oceans,* Royal Meteorological Society, England.

——, and D. S. Shea, 1973: The hurricane inner core region. Part II: Thermal stability and dynamic characteristics. *J. Atmos. Sci.*, **30,** 1565–1576.

Kurihara, Y., and R. E. Tuleya, 1974: Structure of a tropical cyclone developed in a three-dimensional numerical simulation model. *J. Atmos. Sci.*, **31,** 893–919.

Jarvinen, B. R., and C. J. Neumann, 1979: Statistical forecasts of tropical cyclone intensity for the North Atlantic basin. NOAA Tech. Memo. NWS-NHC-10, 22 pp. [NTIS PB297185.]

Neter, J., W. Wasserman and G. A. Whitmore, 1978: *Applied Statistics,* Allyn and Bacon, 743 pp.

Ooyama, K. V., 1982: Conceptual evolution of the theory and modelling of the tropical cyclone. *J. Meteor. Soc. Japan,* **60,** 369–380.

Riehl, H., 1954: *Tropical Meteorology,* McGraw-Hill, 392 pp.

Rodgers, E. B., and R. F. Adler, 1981: Tropical cyclone rainfall characteristics as determined from a satellite passive microwave radiometer. *Mon. Wea. Rev.*, **109,** 506–521.

Rosenthal, L., 1978: Numerical simulation of tropical cyclone development with latent heat release by the resolvable scales. Part I: Model description and preliminary results. *J. Atmos. Sci.*, **35,** 258–271.

Sadler, J. C., 1976: Tropical cyclone initiation by the tropical upper tropospheric trough. *Mon. Wea. Rev.*, **104,** 1266–1278.

Schubert, W. H., and J. J. Hack, 1982a: Inertial stability and tropical cyclone development. *J. Atmos. Sci.*, **39,** 1687–1697.

——, and ——, 1982b: Transformed Eliassen balanced vortex model. *J. Atmos. Sci.*, **40,** 1571–1583.

Steranka, J., E. B. Rodgers and R. C. Gentry, 1984: The diurnal variation of Atlantic Ocean tropical cyclone cloud distribution inferred from geostationary satellite infrared measurements. *Mon. Wea. Rev.*, **112,** 2338–2344.

Willoughby, H. E., J. A. Clos and M. G. Shoreibah, 1982: Concentric eye walls, secondary wind maxima, and the evolution of the hurricane vortex. *J. Atmos. Sci.*, **39,** 395–411.